

Dynamic and scattering properties of the Sierpinski gasket

This article has been downloaded from IOPscience. Please scroll down to see the full text article.

1992 J. Phys.: Condens. Matter 4 3153

(<http://iopscience.iop.org/0953-8984/4/12/011>)

View [the table of contents for this issue](#), or go to the [journal homepage](#) for more

Download details:

IP Address: 171.66.16.159

The article was downloaded on 12/05/2010 at 11:35

Please note that [terms and conditions apply](#).

Dynamic and scattering properties of the Sierpinski gasket

C Benoit, G Poussigue and A Assaf

Groupe de Dynamique des Phases Condensées, UA CNRS 233, Université Montpellier II, Sciences et Techniques du Languedoc, Place E Bataillon, 34095 Montpellier Cédex 5, France

Received 30 May 1991, in final form 21 October 1991

Abstract. The dynamic and scattering properties of the Sierpinski gasket are studied in systems up to as large as $N = 2391\,486$ atoms (level = 13), using the spectral moments method. Two models, with scalar and vectorial forces, are developed. The effects of disorder are also investigated. The density of states on the scalar perfect Sierpinski gasket is found to be in agreement with previous results. For the vectorial perfect model, we find that the density of states exhibits self-similar properties. For the disordered systems, results show that the density of states exhibits two regimes. For the disordered vectorial model, the density of states is proportional to ω in the low-frequency regime. A cross-over is found, and on short length scales the density of states is proportional to ω^d . Determination of the correlation functions shows that, although the density of states follows the Debye law, the low-frequency region does not correspond to an acoustic regime, which is in agreement with the lack of translational invariance. A microscopic theory of the scattering of light by fractals is developed and comparisons with recent results obtained in Raman scattering measurements of silica aerogels are reported. The results confirm that, in the fracton regime, the Raman intensity behaves with a power law, with the value of the exponent depending on the scaling properties and the susceptibility derivatives.

1. Introduction

Self-similar lattices have been the subject of much attention. It has been claimed that the structure of fractals may bridge the gap between crystals or quasi-crystals and disordered materials. From a structural point of view they may serve as simple models for disordered systems such as porous media, polymers, epoxy resins or gels. The most widely studied systems include the Sierpinski gaskets and percolation networks. The density of states on a fractal was studied for the first time by Alexander and Orbach (1982), who took the scaling properties of the mass and the connectivity into account. They found that elastic properties are described by phonons for long wavelengths $\lambda \gg \xi$ where ξ is some 'correlation length', and by localized vibrational states, called fractons, for $\lambda \ll \xi$. More specifically, their studies dealt with the 2D Sierpinski gasket and percolation networks. For the Sierpinski gasket they found that the density of states behaves as ω^{d-1} with the fracton dimensionality

$$\tilde{d} = 2D/(2 + \theta) \quad (1)$$

where D is the fractal dimensionality, and θ is the exponent giving the dependence of

the diffusion constant on distance—or the connectivity. For the Sierpinski gasket $\theta = 0.322$ and $D = \ln 3 / \ln 2 = 1.585$, giving $\tilde{d} = 1.365$.

For the percolation clusters, they suggested that the DOS (real quantum density of states for electrons; density of one-phonon states for vibrations) in all Euclidean dimensions d ($d \geq 2$) obeys the universal law

$$g(\omega) \sim \omega^{\tilde{d}-1} \quad (2)$$

with $\tilde{d} = 4/3$.

For fractals they associated a length scale $L = L(\omega)$ with the vibrations. If we consider a very large fractal, the degrees of freedom will be dN where N is the number of atoms. Now we disconnect this fractal into M identical blobs with size L . Then κdM frequencies of the modes of the large fractal will fall to zero (κ takes into account the rotational degrees of freedom; $\kappa = 3/2$ for the 2D Sierpinski gasket). Let $\omega(L)$ be the lowest non-zero frequency of a blob (and of the large disconnected fractal). The total number of degrees of freedom being constant, the number of missing low-frequency modes is equal to the total number of translational and rotational modes:

$$\int_0^{\omega(L)} g(\omega) d\omega = \kappa dM = \kappa d \frac{Nd}{n(L)} \quad (3)$$

where $n(L)$ is the number of degrees of freedom of a blob. Taking into account the form (2) of $g(\omega)$, and the scaling of the mass $n(L) \sim L^D$ ($n(L) = L^D$ for a large 2D Sierpinski gasket: see equations (11) and (20)), one obtains

$$L^D \omega(L)^{\tilde{d}} = \text{const.} \quad (4)$$

If the system is weakly connected, the density of states and the lower frequencies of blobs are not changed when the blobs are connected. From the relation (4) it is possible to define a localization length for a given low frequency of the large fractal. One obtains

$$L(\omega) \sim \omega^{-\tilde{d}/D}. \quad (5)$$

Now if we consider a dense packing of fractals with size L ($= \xi$), a cross-over will occur for the frequency

$$\omega_\infty \sim L^{-D/\tilde{d}}. \quad (6)$$

For length scales less than L , the solutions exhibit a fractal behaviour, while for larger length scales, the solutions are uniform and an acoustic regime may appear. Let us note that for the percolation clusters the relation (4) is an approximation (Yakubo *et al* 1990).

Simulations have been performed by several groups to verify the 4/3 conjecture and the scaling form of the density of states.

Concerning the percolation networks, which are fractals on smaller length scales than the percolation length ξ_c , simulations have been performed by Derrida *et al* (1984) using an effective-medium approximation (EMA) treatment. They found $\tilde{d} = 1$ but they pointed out that their method does not perform well for determination of the critical exponents. Yakubo and Nakayama (1987, 1989), with a scalar model and using the resonance method of Williams and Maris (1985) on a large network, found a value for \tilde{d} that was very close to 4/3 near ρ_c for the 2D (700^2) lattice (Yakubo and Nakayama 1987) and 3D (70^3) lattice (Yakubo and Nakayama 1989). Webman and Grest (1985), who studied different models for diffusion limited aggregate (DLA) clusters (64^2 lattice),

found that the behaviour of the DOS largely depends on the type of forces. In another paper (Grest and Webman 1984) they used an 18^3 cubic lattice and found a dimensionality value close to $4/3$. Feng and Sen (1984) studied a triangular percolating network with central and non-central forces. They did not determine the DOS of these systems but also found that the critical exponents depend on the type of forces. Feng (1985) noted that the elasticity of a tenuous material should be dominated by stretching at small scales and by bending at larger ones, producing an additional cross-over. Visualizations of fractons have been presented by Courtens *et al* (1989).

Studying the perfect and the disordered Sierpinski carpet, Bourbonnais *et al* (1989) obtained a fracton dimensionality equal to 1.6, very different from $4/3$. Numerical studies were performed on samples of 4096 atoms on a parallel experimental computer.

Concerning Sierpinski gaskets, the first results on energy levels of a tight-binding Hamiltonian with a magnetic field have been discussed by Rammal and Toulouse (1982). Using a decimation process, Domany *et al* (1983), Alexander (1983a, b) and Alexander and Haveli (1983) obtained the density of states of the Sierpinski gasket and of several other self-similar structures. The energy levels were discrete, very closely spaced, highly degenerate and exhibited self-similarity. Using renormalization of the equations of motion, Rammal and Toulouse (1983) and Rammal (1984) investigated the density of states of d -dimensional Sierpinski gaskets. They showed that for $d > 1$ the spectral measure is a superposition of two distinct pure point measures of relative weights $d/(d+1)$ and $1/(d+1)$. The first type concerns localized states while the second concerns hierarchical states, localized around the holes of the gasket. The density of states has also been investigated by Tremblay and Southern (1983) using direct-space renormalization techniques. Their results are in agreement with previous studies.

Concerning localization of the modes Grest and Webman (1984) found that, whereas all states in the Debye regime are extended, a considerable fraction of the states in the fracton regime also seem to be extended. Southern and Douchant (1985), studying fractal lattices, found evidence for the existence of extended and localized states at high frequencies.

It has also been suggested that the fractons are superlocalized (Levy and Souillard 1987, Brook Harris and Aharony 1987). This means that they decay faster than exponentially with distance, namely as

$$\Psi(r) \sim \exp\{-[r/\xi(\omega)]^{\bar{a}}\} \quad (7)$$

where $\xi(\omega)$ is the localization length and $\bar{a} = 1$ for the classical Anderson localization.

In numerical studies in a 2D percolation network, De Vries *et al* (1989), using a 200^2 lattice, determined that the superlocalization component cannot be larger than $\bar{a} = 1.1$, while Yakubo and Nakayama (1989) found a value of $\bar{a} = 2.3$, which is not consistent with any theoretical predictions. Bourbonnais *et al* (1989) found no evidence to support the conjecture of superlocalization.

Existence of a steepness in the cross-over region of the density of states in percolating clusters has been discussed at length by several authors, such as Derrida *et al* (1984), Yakubo and Nakayama (1987) and Grest and Webman (1984), with contradictory results. Identifying the maximum frequency of the lowest acoustic branch with the cross-over frequency ω_c , Southern and Douchant (1985) found no sharp structure and a smooth cross-over between a phonon and fracton regime in the DOS.

On the other hand, recent experimental investigations, i.e. small-angle neutron scattering (SANS) (Vacher *et al* 1987, Schaeffer and Keefer 1986) and small-angle x-ray scattering (SAXS) (Dos Santos *et al* 1987), demonstrated that silica aerogels are excellent

examples of porous solids having a fractal structure at length scales L larger than particle size a ($\approx 30\text{--}50$ Å for a material with a density 0.015 g cm^{-3} , $D = 1.8$) and smaller than correlation length ξ ($\approx 500\text{--}1000$ Å for the same material). In such materials three vibration regimes can be expected:

- (i) waves of wavelength $\lambda > \xi$ ($\omega < \omega_\xi$) are weakly localized acoustic phonons;
- (ii) with increased frequency, a new regime occurs beyond the first cross-over frequency ω_{col} , the new excitations being called fractons; and
- (iii) as the frequency is further increased, a second cross-over is reached at ω_{co2} and the vibration spectrum is dominated by bulk and surface modes.

Below a and above ξ , the material is homogeneous (Vacher *et al* 1987).

Experimental investigations of light scattering from silica aerogels by Courtens *et al* (1987, 1988), Tsujimi *et al* (1988), Pelous *et al* (1990) and Vacher *et al* (1990) constitute a very detailed test of the scaling considerations of the fracton model. Investigations of the vibrational dynamics of these materials have shown evidence of a cross-over from long-wavelength acoustic phonons to fractons in the Brillouin scattering frequency range. Scattering from fractons was observed in the very low-frequency Raman region. The authors show that in a large frequency range the intensity of the scattered light follows a power law

$$I(\omega)/n(\omega) \sim \omega^{-\alpha} \quad (8)$$

with $\alpha \approx 0.36\text{--}0.39$ for the samples studied, where $n(\omega)$ is the Bose–Einstein factor. The scattering of light from aerogels has been discussed by Alexander (1989) using scaling arguments. He found a power law for the scattering by fractons but concluded that α cannot be easily related to the spectral dimension but rather to the exponent σ that characterizes the scaling form for the strains. Some numerical studies of Raman scattering from fractals have been performed by Montagna *et al* (1990) on square (65×65) and cubic ($29 \times 29 \times 29$) site percolation lattices using diagonalization of the dynamical matrix.

It is clear that the dynamics and scattering properties of fractals are still an open question and it would be interesting to investigate very large systems with a method that takes into account the exact structure of the system and the exact values of eigenmodes.

Recently, we found that the spectral moments method could provide the exact response function of very large harmonic systems, whatever the structure, the type of the forces and the dimension (Benoit 1987, 1989, Benoit and Poussiguet 1989). This method has been used for the study of the dynamics of quasi-crystals (Benoit *et al* 1990) and polythiophene (Poussiguet and Benoit 1990, Poussiguet *et al* 1991). More recently we have shown that, with some variations, this method could provide the DOS with good accuracy and the displacement correlation functions of the system.

The method consists of determining the moments of the response functions directly from the dynamical matrix: for instance the dielectric susceptibility of the system if we are studying infrared absorption, or the differential cross section if we are studying inelastic scattering of light or neutrons by the vibrations. Then, using Stieltjes inversion formula, it is possible to compute the response function from the moments. The method is simple and exact. To determine the moments of the response functions, we assume that the coupling between the perturbing field and the sample is applied through local atomic coefficients: ionic charges for infrared absorption, local susceptibility derivative tensors for Raman scattering, Fermi length for inelastic neutron scattering. Furthermore, it is well known that incoherent neutron scattering could provide the DOS of the

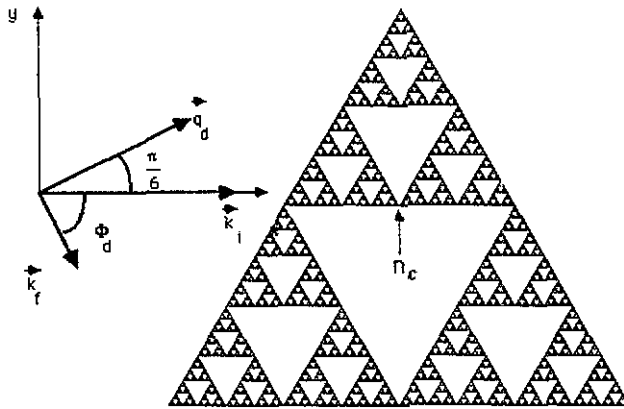


Figure 1. The 2D Sierpinski gasket at stage $n = 8$: the system is built with 9843 atoms; n_c is the 'centre' of the gasket (from Barnsley *et al* 1988). k_i , k_r are the wavevectors of the incident and scattered light respectively, and q_d the momentum transfer.

system. Also it is sufficient in our method to assume that the nuclear Fermi lengths are random variables to obtain the DOS to a good approximation. With small size matrix, it is necessary to average over several systems. Technical details can be found in Benoit *et al* 1992).

In the following we report, for the first time, a computation of the density of states, localization of the fractons and the Raman intensity up to the stage $n = 12$ of perfect and disordered scalar and vectorial models of a 2D Sierpinski gasket. We can compute until stage $n = 13$ (size of the gasket = 2391 486 atoms, computing time 20 min on an IBM 3090-600VF). However, as the results are very close to those obtained with $n = 12$, we restricted our computations to gaskets from stage $n = 2$ to stage $n = 12$, to limit the computing time.

To construct the 2D Sierpinski gasket, we begin with a triangle at stage $n = 0$. The stage $n + 1$ is obtained by juxtaposition of three stage- n structures at the corner (figure 1). The total number of sites at stage n is given by

$$N_n = 3(1 + 3^n)/2. \tag{9}$$

We assume now that atoms or aggregates with mass m are placed at the sites of the gasket and connected by springs.

In the first model (scalar model), we assume that displacements of the particles are represented by a scalar: for instance, motion in a direction orthogonal to the plane of the gasket. Then the set of equations of motion for site n is given by

$$m\ddot{U}_i = -\sum_j k_{ij}U_j \quad \text{with} \quad k_{ii} = -\sum_{j \neq i} k_{ij} \tag{10}$$

where j denotes a neighbouring site of i and k_{ij} are the force constants between the atoms i and j .

Concerning the vibrations, this model does not correspond closely to any known physical situation. However, the resolution of the Schrödinger equation for electrons in the tight-binding model can be described by the same type of equations. This is the only model of the Sierpinski gasket until now. In order to determine the effect of the disorder that appears in real materials, we also studied a model with random force constants.

In the second model (vectorial model) we suppose that the atoms interact with central forces between first neighbours. If two atoms interact with the potential energy $V_{nn'}(r)$, where r is the distance between them, the force constants are given by (Born and Huang 1956, Maradudin et al 1971):

$$\Phi_{\alpha\beta}(n, n') = [(r_{\alpha}r_{\beta}/r^2)((1/r)\delta V_{nn'}/\delta r - \delta^2 V_{nn'}/\delta r^2) - \delta_{\alpha\beta}(1/r)\delta V_{nn'}/\delta r]_{r=r_n^0-r_{n'}^0} \tag{11}$$

The potential energy is given by the harmonic approximation:

$$V = \frac{1}{2} \sum_{\alpha,\beta,n,n'} \Phi_{\alpha\beta}(n, n')u_{\alpha}(n)u_{\beta}(n') \tag{12}$$

where r_n^0 is the equilibrium position and $u_{\alpha}(n)$ the Cartesian α component of the displacement of the n th atom. We chose the following form for the potential energy:

$$V_{nn'}(r) = \frac{1}{2}k_{nn'}(r - r_{nn'}^0)^2 \tag{13}$$

where $r_{nn'}^0$ is the distance between atoms n and n' . With this simple model the first derivative in the relation (11) is equal to zero.

In the perfect models, the force constants and the masses are taken as being equal to 1. For the disordered models, the force constants are given as

$$k_{ij}^R = k_{ji}^R = k_{ij}\gamma_{ij} \quad j > i \quad (\text{scalar model}) \tag{14}$$

and

$$\begin{aligned} \Phi_{\alpha\beta}^R(n, n') &= \Phi_{\beta\alpha}^R(n', n) = \Phi_{\alpha\beta}(n, n')\gamma_{\alpha\beta}(n, n') \\ (\beta, n') &> (\alpha, n) \quad (\text{vectorial model}) \end{aligned} \tag{15}$$

where the γ_{ij} and $\gamma_{\alpha\beta}(n, n')$ are random variables distributed according to the continuous bounded probability density functions $P(\gamma_{ij})$ and $P(\gamma_{\alpha\beta}(n, n'))$. $P(\gamma)$ is identical to zero except in a region $0 < \gamma < 1$. We investigated numerically the class for $P(\gamma) = 1$. It should be noted that the disordered vectorial model is now not strictly a central force type. The translational invariance of the gasket as a whole was always taken into account.

2. Density of states

To test the accuracy of the spectral moments method, we first compared the results of this technique for the perfect scalar model and the exact results obtained by the decimation process developed by Domany et al (1983). In this paper, the authors showed that the energy of states of the system at level n can be calculated from those of the system at level $n - 1$ by

$$\varepsilon_n = [-3 + (9 - 4\varepsilon_{n-1})^{1/2}]/2 \tag{16}$$

or if we work with the square of the frequencies ($\varepsilon = \omega^2 - 4$)

$$\omega_n^2 = [5 + (25 - 4\omega_{n-1}^2)^{1/2}]/2 \tag{17}$$

in agreement with the result of Rammal and Toulouse (1983).

Table 1. Comparison between the exact frequencies (left column) obtained by using the decimation process and the values obtained by the spectral moments method (right column) with random charges on atoms. Gasket at stage $n = 12$, 180 generalized moments, with averages over two systems.

Decimation method	Moments method
1.381 96	1.381 97
0.697 22	0.697 43
0.293 64	0.293 76
0.143 56	0.143 55
0.059 36	0.059 43
0.028 87	0.028 88
0.011 78	0.011 56
0.006 06	0.005 99
0.001 18	0.001 19

Starting from

$$\omega_{n-1}^2 = 3$$

one obtains the 'descendent' values

$$(5 + \sqrt{13})/2 \dots$$

which are called 'mid-gap states' by Domany *et al*, and starting from

$$\omega_{n-1}^2 = 5$$

one obtains the states

$$(5 + \sqrt{5})/2 \dots$$

which form the edges of the gap intervals.

These exact values are compared with the values obtained by the moments method in table 1. We observe that an excellent agreement is obtained, which is quite remarkable, especially for the low-frequency region. However, for the very low-frequency part of the DOS ($u/u_{\max} < 10^{-4}$, $u = \omega^2$) and with very large systems ($n \geq 7$), the moments method could not resolve the spectrum and provided only an average value.

The computations were performed from level $n = 2$ to level $n = 12$. When the size of the matrix was not very large it was necessary to compute an average over several systems. For the perfect scalar models the results are reported in figures 2 and 3. The DOS of the $n = 12$ lattice is reported in linear scale in figure 2 and is in complete agreement with the exact DOS obtained by the decimation process (Domany *et al* 1983) or by renormalization methods (Tremblay and Southern 1983). We report the log-log plot of the DOS in figure 3 for stages $n = 5, 8$ and 12. In addition, we can easily see that the density of states exhibits some self-similarity. The low-frequency part of the spectrum is not as rich in structure as the high-frequency part. Two reasons can be given: for small systems, there are few modes in this region, and for large systems, the resolution of the moments method does not allow separation of the different peaks. However, we note that as n increases the number of modes in the low-frequency part increases strongly (figure 3(b)) but without any effect of self-similarity. Only for large n does the low-frequency part begin to exhibit some self-similarity (figure 3(c)).

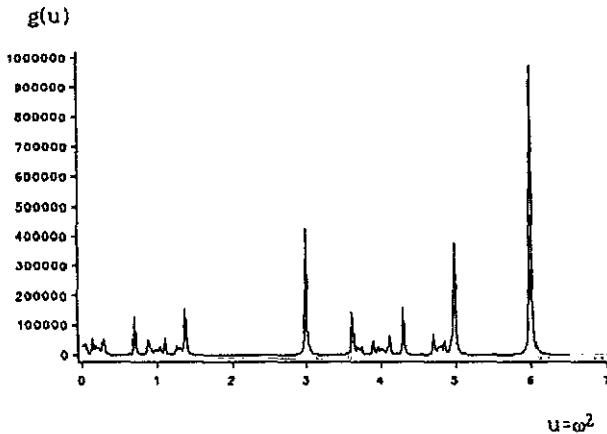


Figure 2. Linear plot of the density of states for the scalar model of the perfect Sierpinski gasket for the $n = 12$ level.

With the perfect scalar model, the mode at $u = 6$ exhausted one-third of the total DOS. The calculations reported in figure 3 do not seem to agree with this result. However, we calculated the integrated density of states with a linear plot and found the $u = 6$ mode with the right weight. Thus we conclude that, if the log-log type of plot has the advantage of expanding the very low-frequency part of the spectrum and revealing easily whether the spectrum obeys to a simple power law, it has the great disadvantage of squeezing the curves.

We report in figure 4 the frequencies of the fracton that is here the mode with the lower frequency plotted as a function of the size of the gasket. These frequencies, following Alexander and Orbach (1982), must fit equations (2) or (6). In the Sierpinski gasket the size L is such that

$$L = 2^n r^0 \quad (18)$$

where r^0 is the distance between the atoms. From (2) and (6) one obtains the following relation:

$$\ln \omega_{\infty}^2 = -[(2 + \theta) \ln 2]n + C = -[(2d/\bar{d}) \ln 2]n + C \quad (19)$$

where C is a constant depending on r^0 and θ .

We note that from $n = 2$ to $n = 6$ the points followed a straight line (figure 4). For $n \geq 7$ the frequencies were too low for the method. The slope of the line gave $\theta = 0.234$, which is not far from the value of Alexander and Orbach ($\theta = 0.322$). From this value we obtain the fracton dimensionality $\bar{d} = 1.418$, not very different from the theoretical value $\bar{d} = 1.365$. The values of the spectral dimensionality obtained from the fracton dispersion or from the slope of the DOS in the fracton regime are reported in table 2.

For the disordered model, the results are reported in figure 5, for one stage ($n = 12$). The results are somewhat surprising. For quite large systems we note that the spectrum has a tendency to exhibit two regions: a low-frequency regime where the DOS presents some similarity with the DOS of the perfect model, and a high-frequency regime where the DOS is proportional to ω^{d-1} with a slope equal to 0.49 giving $\bar{d} = 1.49$. We investigated numerically a different class of probability density, such that

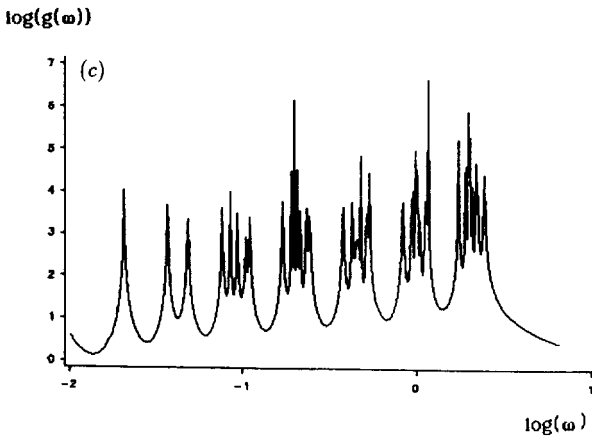
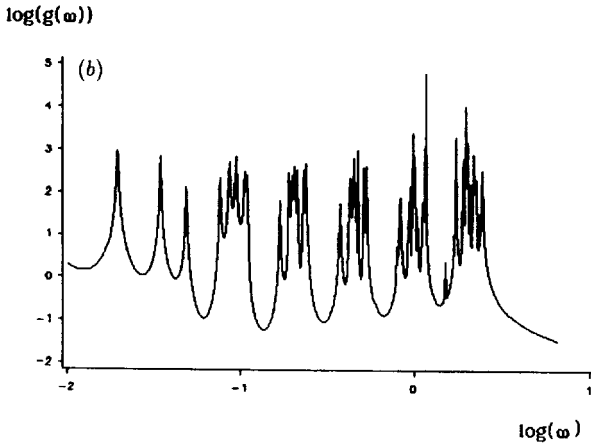
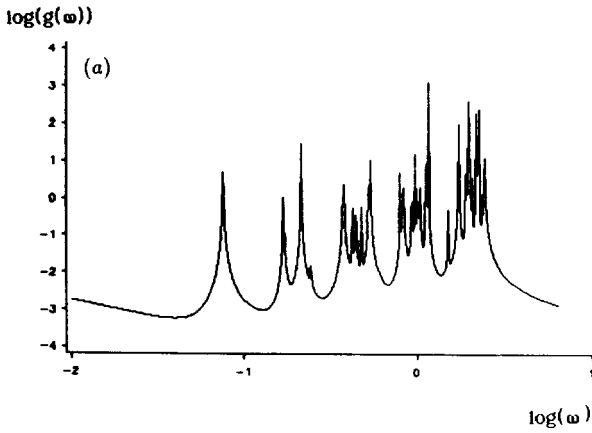


Figure 3. Log-log plot of the density of states for the scalar model of the perfect Sierpinski gasket for the (a) $n = 5$, (b) $n = 8$ and (c) $n = 12$ levels.

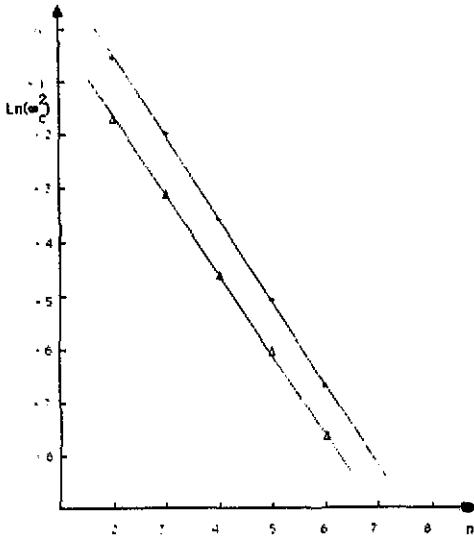


Figure 4. Logarithm of the square of the lowest frequencies of the spectral density of the scalar perfect Sierpinski gaskets (*) and logarithm of the square of the averaged lowest frequencies of the spectral density of the disordered models (Δ) plotted as a function of the level n of the gasket from $n = 2$ to $n = 6$. For $n \geq 7$ it is not possible to determine the lowest frequency with the moments method.

Table 2. Values of the fracton dimensionality \bar{d} obtained with the different models from the fracton dispersion (a) and from the slope of the DOS in the fracton regime (b).

	Scalar model		Vectorial model	
	Ordered	Disordered	Ordered	Disordered
(a)	1.418	1.51	1.238	—
(b)	—	1.49	—	1.48

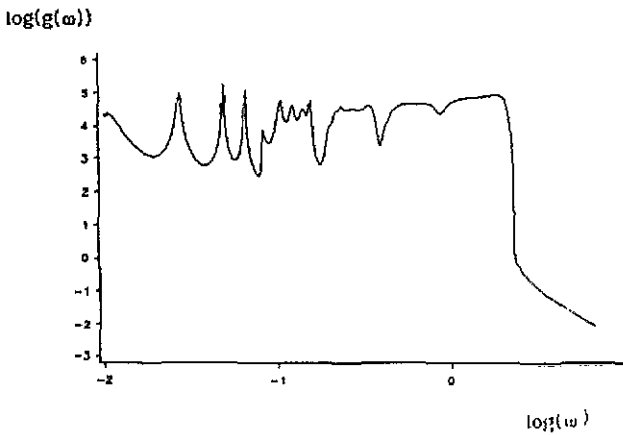


Figure 5. Log-log plot of the density of states for the disordered scalar Sierpinski gasket for the $n = 12$ level.

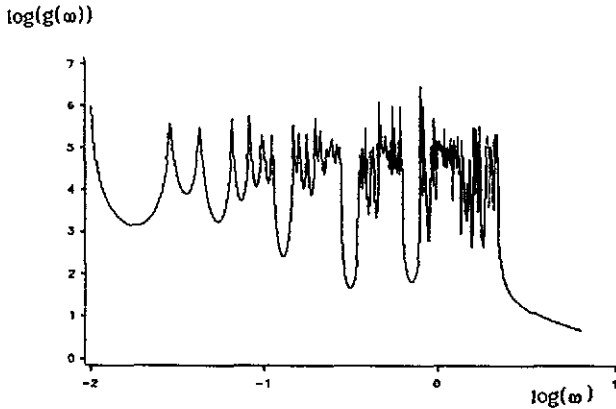


Figure 6. Log-log plot of the density of states for the vectorial model of the perfect Sierpinski gasket for the $n = 12$ level.

$P(\gamma) = 1$ for $0.5 < \gamma < 1.5$ and we did not find any significant change. As for the perfect gasket, we calculated the dispersion of the fracton frequencies. However, for small gaskets the lowest frequency fluctuated. So the value for the lowest frequencies was averaged over 60 gaskets for $n = 2$ and $n = 3$, 40 gaskets for $n = 4$, 25 gaskets for $n = 5$ and 14 gaskets for $n = 6$. The results are reported in figure 4. From $n = 2$ to $n = 6$ the points follow a straight line. The slope of the line gave $\theta = 0.10$. From this value one obtains the fracton dimensionality $\bar{d} = 1.51$. We note that the value of the fracton dimensionality obtained from the fracton dispersion (2) was in agreement with the value obtained from the slope of the DOS in the fracton regime.

For the perfect vectorial model, the results are reported in figure 6 for one stage ($n = 12$). We observe that, as for the scalar model, for large systems, the density of states exhibited some self-similarity. However, there is a large region in the high-frequency part of the spectrum that was not self-similar. This effect was also observed for the scalar model but for a smaller region of the spectrum. The frequencies of the fracton as a function of the size of the gasket are reported in figure 7. The slope of the line gave $\theta = 0.59$. The fracton dimensionality was $\bar{d} = 1.223$, very different from the value obtained with the scalar models.

In order to study the dynamics of the vectorial model in detail, we used the group theory. The method used for the block diagonalization of the dynamical matrix is based on a paper of Maradudin and Vosko (1968). This is done by constructing a set of matrices $U(R)$ where R is a symmetry operation of the group of the system. Furthermore, combination of these matrices with irreducible representations leads to the form of symmetry-adapted functions. One can further simplify the form of the dynamical matrix. Irreducible representations are A_1 , A_2 and E for the C_{3v} group.

The gasket at stage n presented $3(3^n + 1)$ degrees of freedom. Decomposition of the representation given by the motion into irreducible representations gave

$$\Gamma_n = \frac{1}{2}(3^n + 1)A_1 + \frac{1}{2}(3^n + 1)A_2 + (3^n + 1)E. \tag{20}$$

Block diagonalization was performed only for gaskets up to the $n = 6$ level in order to limit the computing time and the DOS for each symmetry was computed by the moments method.

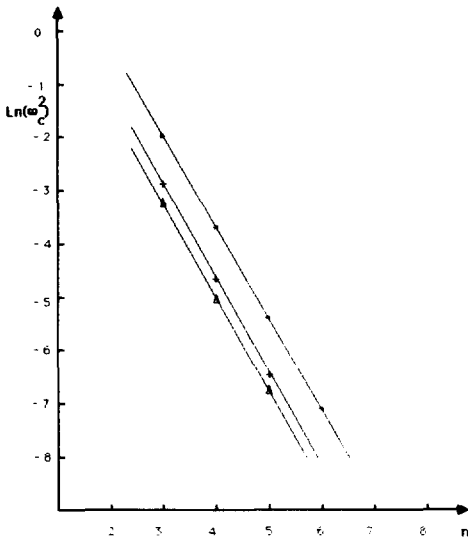


Figure 7. Logarithm of the square of the lowest frequencies of the spectral density of the vectorial perfect Sierpinski gaskets plotted as a function of the level n of the gasket. We have reported the fracton dispersion for three symmetries: the frequencies of the E type fractons (Δ) being the lowest, the curve is the same as the one obtained with the non-block-diagonalized matrices. Crosses (+) and stars (*) give the dispersion for the A_1 and A_2 type fractons.

The results are reported in figure 8 at level $n = 6$ for the three symmetries. The DOS presented some self-similarity. The frequencies of the fractons as a function of the size of the gasket are reported in figure 7. Exactly the same slope was found for the three symmetries (fractons A_1 , A_2 and E). This result confirms that the values of θ and \bar{d} depended only on the model and not on the symmetry of the fracton.

The results for the disordered vectorial lattices are reported in figure 9 for the three levels ($n = 5, 8$ and 12). For quite large systems we note that the spectrum exhibits a real 'phonon regime' with a slope very close to 1 (≈ 1.001) for $\omega < \omega_c$ ($\omega_c \approx 0.1$), and a 'fracton regime' ($\omega > \omega_c$) where the DOS is proportional to $\omega^{\bar{d}-1}$ with a slope equal to 0.48 which gives $\bar{d} = 1.48$ (table 2). The cross-over between the two regimes is smooth and presents a small hump. These spectra are analogous to the spectra obtained for the percolating network with a concentration above p_c (Yakubo and Nakayama 1987, 1989, Grest and Webman 1984). The frequency ω_c did not change with the size of the gasket. However, from the lack of translational invariance the low-frequency regime cannot be a Debye regime. This result will be confirmed by the study of the localization of the eigenmodes. We also considered a Gaussian distribution for $P(\gamma)$ with a strong dispersion for the probability density. The results were in complete agreement with previous results.

Concerning dispersion of the fractons, we could not obtain a clear behaviour of the lowest frequencies with the size of the gaskets, even by using a statistical average over 100 systems. We believe that such a result is due to a strong localization of the modes. We shall return later to this question. In order to clarify the effect of the disorder, we determined the position correlation functions of the systems.

3. Localization

The time-dependent position correlation function is given by

$$G_{\alpha\beta}(n, n', t) = \langle\langle (u_\alpha(n, t)u_\beta(n', 0)) \rangle\rangle \quad (21)$$

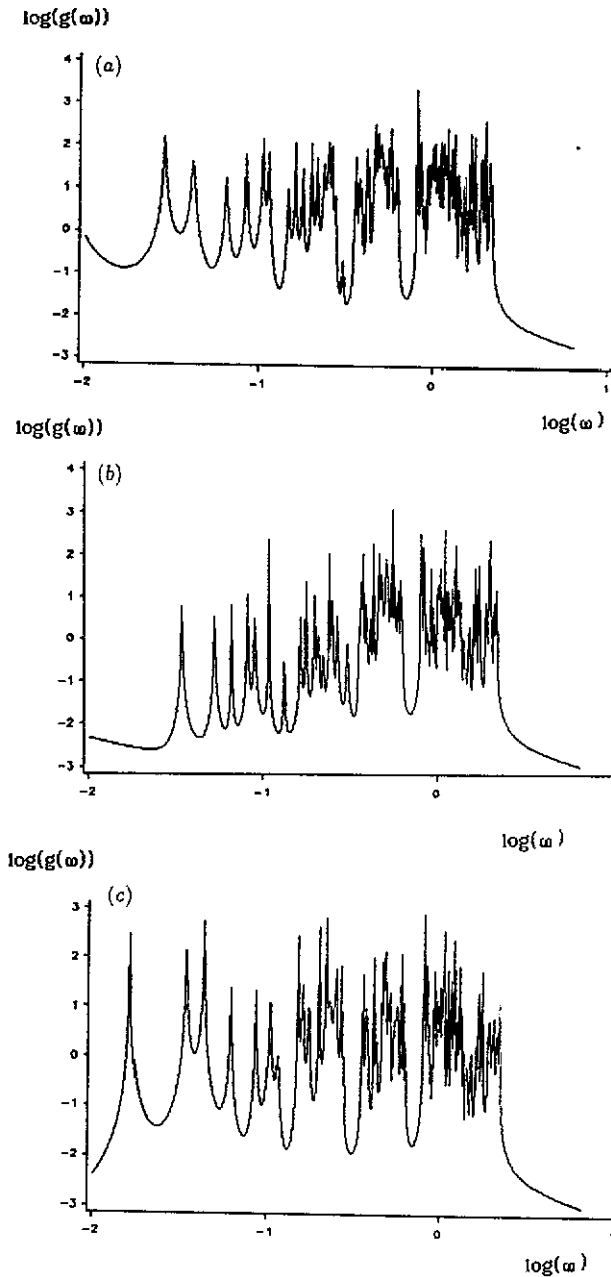


Figure 8. Log-log plot of the density of states with the (a) A_1 symmetry, (b) A_2 symmetry and (c) E symmetry (level $n = 6$).

with

$$\langle A \rangle = (1/Z) \text{Tr}(e^{-\beta H} A) \tag{22}$$

and H is the Hamiltonian of the system, Z the partition function and $u_\alpha(n, t)$ the

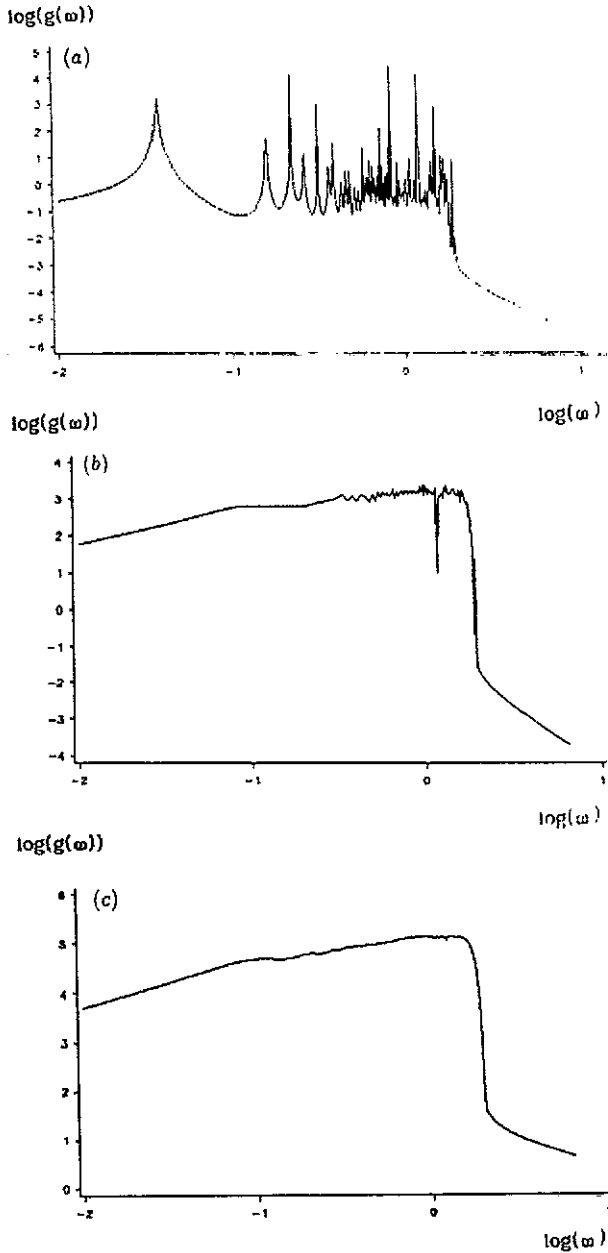


Figure 9. Log-log plot of the density of states for the vectorial model of the disordered Sierpinski gasket for the (a) $n = 5$, (b) $n = 8$ and (c) $n = 12$ levels.

Cartesian α component of the displacement of the n th atom in the Heisenberg representation.

The imaginary part of the Fourier transform of $G_{\alpha\beta}(n, n', t)$ is given by

$$G_{\alpha\beta}(n, n', \omega) = 2\pi\hbar[n(\omega) + 1] \sum_j \frac{e_{\alpha n}(j) e_{\beta n'}(j)}{\sqrt{m_n} \sqrt{m_{n'}}} \frac{1}{2\omega_j} [\delta(\omega - \omega_j) - \delta(\omega + \omega_j)] \quad (23)$$

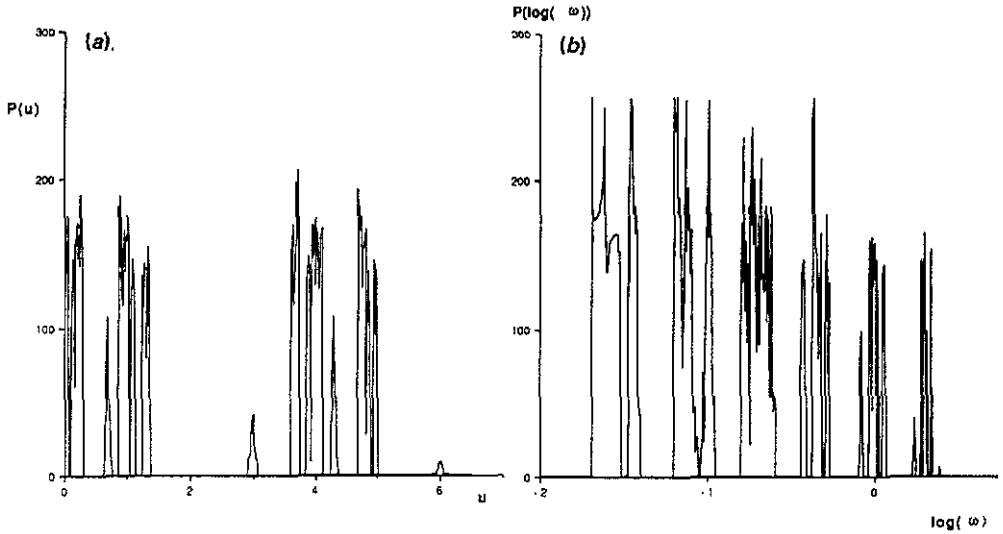


Figure 10. Localization ratio of the modes for the scalar perfect Sierpinski gasket (stage $n = 8$) plotted (a) as a function of the square of the frequency and (b) as a function of the logarithm of the frequency.

where ω_j and $e_{\alpha n}(j)$ are the frequency and the amplitude of the mode j . The physical interpretation of this correlation function is simple only in the classical limit (Maradudin 1969). This function can be understood as being due to the influence of the atom n on the atom n' . If this function vanishes for any frequency this means that there is no correlation between the atoms n and n' . The direct computation of $G_{\alpha\beta}(n, n', \omega)$ presents some difficulties. It is preferable to work with the following function (Benoit 1987):

$$\begin{aligned} \sigma_{\alpha\beta}(n, n', \omega) &= \sum_j \frac{e_{\alpha n}(j) e_{\beta n'}(j)}{\sqrt{m_n} \sqrt{m_{n'}}} \frac{1}{2\omega_j} [\delta(\omega - \omega_j) + \delta(\omega + \omega_j)] \\ &= \sum_j \frac{e_{\alpha n}(j) e_{\beta n'}(j)}{\sqrt{m_n} \sqrt{m_{n'}}} \delta(u - \lambda_j) = S_{\alpha\beta}(n, n', u) \end{aligned} \tag{24}$$

with $u = \omega^2$ and $\lambda_j = \omega_j^2$, which is identical to $2\pi\hbar[n(\omega) + 1]^{-1}G_{\alpha\beta}(n, n', \omega)$ for $\omega > 0$, symmetrical and independent of the temperature. $S_{\alpha\beta}(n, n', u)$ is a particular form of the response function and the spectral moments method can be applied. We observe that for a given frequency ω (or u), the function $S_{\alpha\beta}(n, n', u)$ is proportional to the wavepacket amplitude of the modes centred on ω (or u). We used the relation (24) to calculate the ratio of the second and fourth moments of the spatial distribution of the amplitude. Let us define

$$\mu_2(u) = \sum_{n'} |S_{\alpha\beta}(n, n', u)| |r_{n'} - r_n|^2 \tag{25}$$

$$\mu_4(u) = \sum_{n'} |S_{\alpha\beta}(n, n', u)| |r_{n'} - r_n|^4. \tag{26}$$

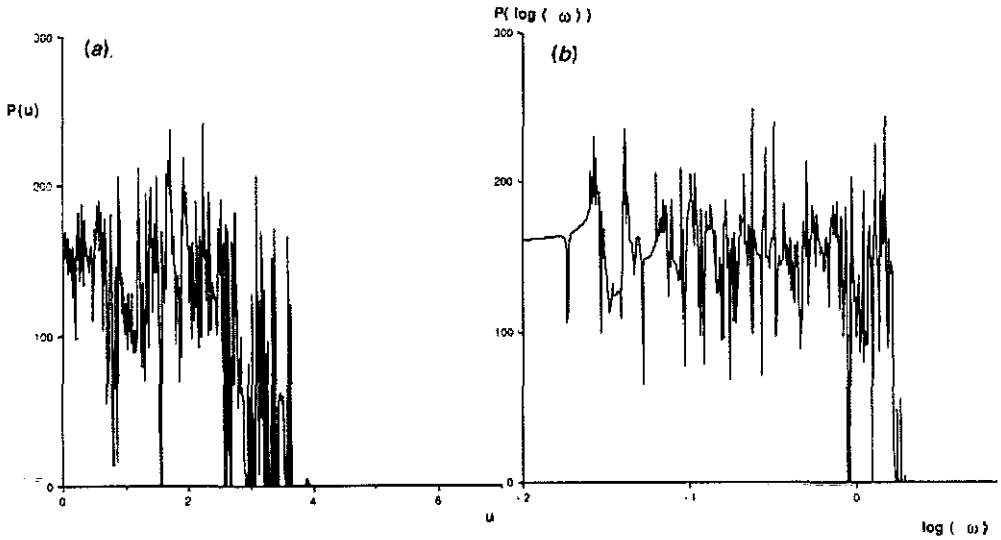


Figure 11. Localization ratio of the modes for the scalar disordered Sierpinski gasket (stage $n = 8$) plotted (a) as a function of the square of the frequency and (b) as a function of the logarithm of the frequency.

Here $|S_{\alpha\beta}(n, n', u)|$ is the absolute value of function $S(n, n', u)$ for the scalar model or the square root of the sum of the squares of the diagonal elements of function $S_{\alpha\beta}(n, n', u)$. Then the localization ratio is

$$P(u) = \mu_4(u)/\mu_2(u). \quad (27)$$

This ratio gives the magnitude of the extension for the modes that concern the atom n . Here the atom n was always the atom n_c of the 'centre' of the gasket (see figure 1). In order to limit the computing time we operated with the stage $n = 8$ gasket and the atoms n' were the 80 first neighbours of atom n_c . Results are reported in figures 10–13 in linear u plot (a) and $\log(\omega)$ plot (b). We observe that for all models the high-frequency modes are much more localized than the low-frequency ones. We shall now consider the scattering properties of the gasket.

4. Light scattering

The diffusion of light is usually obtained with the help of macroscopic Maxwell equations where the fields are averaged over a volume ΔV that is small but large enough, however, to contain very many atoms and molecules (Jackson 1962). Such an approach is not possible in fractal systems where the average of physical quantities (density is a well known example) is strongly dependent on the value of the volume ΔV . It is necessary, therefore, to develop a more microscopic approach where the atomic structure is taken into account exactly.

In the following, we show how, by using the spectral moments method, we can calculate the Raman scattering spectra of fractals. Then we apply the method to the Sierpinski gasket. This model is certainly not the best for comparison with the experimental data. However, it could provide interesting indications on the behaviour

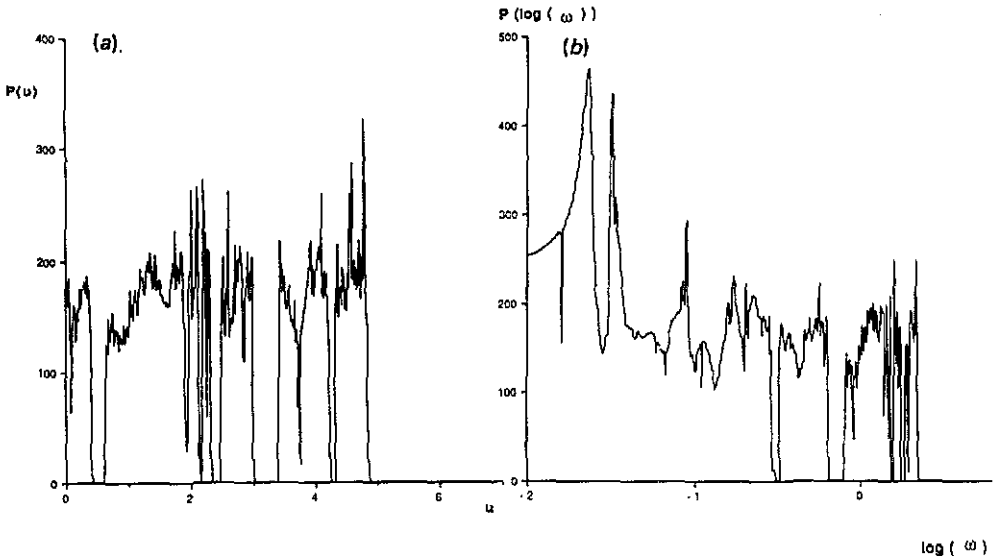


Figure 12. Localization ratio of the modes for the vectorial perfect Sierpinski gasket (stage $n = 8$) plotted (a) as a function of the square of the frequency and (b) as a function of the logarithm of the frequency.

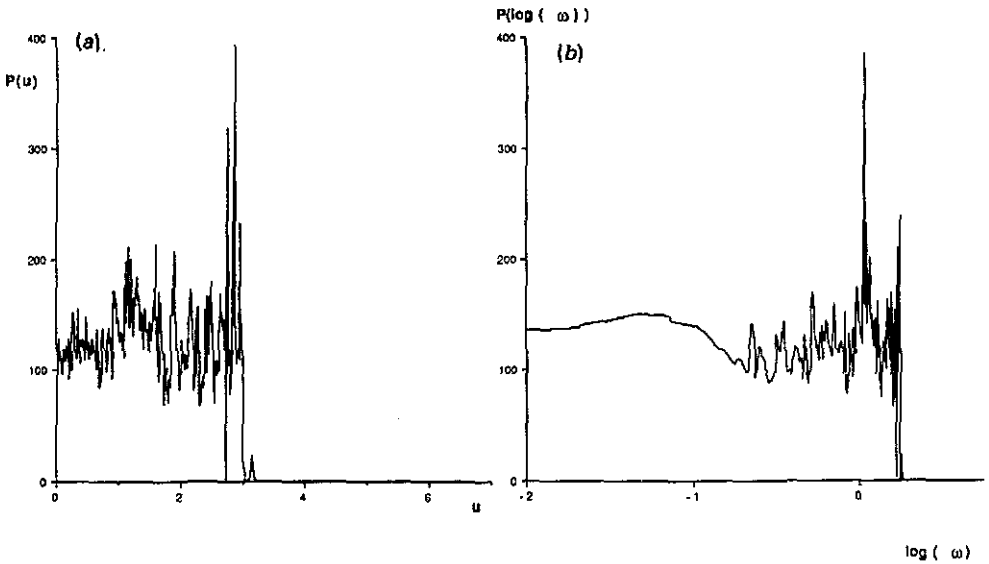


Figure 13. Localization ratio of the modes for the vectorial disordered Sierpinski gasket (stage $n = 8$) plotted (a) as a function of the square of the frequency and (b) as a function of the logarithm of the frequency.

of the scattering spectrum and it provides a good illustration of the technique. We have computed the spectra with a disordered vectorial model, which seems to be closer to physical situations. In this simple model, we do not take into account the

polarization effects. To introduce our computing method, we first mention some results concerning light scattering.

The time average of the power flux of the scattered light with a frequency between ω_i and $\omega_i + d\omega_i$ crossing the surface dS at distance r from the scattering centre is given by (Hayes and Loudon 1978, Jackson 1962, Chu 1974, Lax and Nelson 1971):

$$dQ_d = \frac{1}{\mu_0} \frac{V}{2\pi} \frac{E_i^2}{r^2} \frac{\omega_i^2}{c} \int_{-\infty}^{\infty} \langle g(r, t)g(r, t + \tau) \rangle e^{i\omega_i \tau} \sin^2 \Phi d\tau dS d\omega_i$$

with

$$g(r, t) = (1/\sqrt{V})(r/E_i)A(r, t) \quad (28)$$

where ω_i is the frequency of the scattered light, Φ the angle between the polarization of incident light and the direction of propagation of the scattered field, E_i the amplitude of the incident electric field and $A(r, t)$ the amplitude of the vector potential of the scattered electromagnetic field. V is the scattering volume.

The vector potential $A(r, t)$ is given by

$$A(r, t) = \frac{\mu_0}{4\pi} \int \frac{\delta(t - t' - |r - r'|/c)}{|r - r'|} \frac{\partial P(r', t')}{\partial t'} dr' dt' \quad (29)$$

where $P(r, t)$ is the macroscopic dielectric polarization. This quantity is the average over a volume ΔV of the microscopic polarization P_m of the medium

$$P(r, t) = \frac{1}{\Delta V(r)} \int_{\Delta V(r)} P_m(r', t) dr' \quad (30)$$

The microscopic polarization is given by

$$P_m(r, t) = \sum_i q_i u_i(t) \delta(r - r_{0i}) \quad (31)$$

where u_i is the displacement of the charge q_i relative to the equilibrium position r_{0i} .

As already mentioned, in fractal materials this definition cannot be applied because the value of the polarization depends on the value of the volume ΔV . To avoid this difficulty, we chose ΔV for the volume of the homogeneous particles.

If $E_i(r, t)$ is the incident field with frequency ω_i and wavevector k_i , the induced polarization is given by

$$P(r, t) = \varepsilon_0 \chi(r, t) E_i \exp[i(k_i \cdot r - \omega_i t)] \quad (32)$$

where $\chi(r, t)$ is the dielectric susceptibility. In this simple model we assume that the vector P is in the same direction as the vector E . In the homogeneous medium, the intensity of the scattered light is obtained by expanding fluctuations of the susceptibility in plane waves (phonon series) with frequency $\omega_j(q_{ph})$ and wavevector q_{ph} . In a very porous material, where the density is not homogeneous on the scale of a fraction of a wavelength, the problem of determining $\chi(r, t)$ is much more complicated (Alexander 1989). Fluctuations of the susceptibility $\delta\chi(r, t)$ can be expressed as an expansion in terms of the normal coordinates Q_j . The normal coordinates being a linear combination of the particle displacements $u_\alpha(n)$, the susceptibility can be expanded directly in terms of $u_\alpha(n)$. One obtains

$$\delta\chi(\mathbf{r}, t) = \sum_{\alpha, n} \left(\frac{\partial\chi(\mathbf{r})}{\partial u_\alpha(n)} \right)_0 U_\alpha(n, t) = \sum_{\alpha, n} \chi_{\alpha n}(\mathbf{r}) u_\alpha(n, t). \tag{33}$$

Since the average is calculated over the volume ΔV of the particles, the polarizability and susceptibility must be written only as a function of the mean particle positions $P(\mathbf{r}, t) = P(\mathbf{r}_n, t)$ and $\chi_{\alpha n}(\mathbf{r}) = \chi_{\alpha n}$. The fluctuations of the polarizability are now written as

$$\delta P(\mathbf{r}_n, t) = \varepsilon_0 \delta\chi(\mathbf{r}_n, t) \mathbf{E}_i \exp[i(\mathbf{k}_i \cdot \mathbf{r}_n - \omega_i t)]. \tag{34}$$

Then one obtains for the vector potential

$$\mathbf{A}(\mathbf{r}, t) = \frac{\mu_0}{4\pi} \Delta V \sum_{n'} \int \frac{\delta(t-t' - |\mathbf{r} - \mathbf{r}_{n'}|/c)}{|\mathbf{r} - \mathbf{r}_{n'}|} \frac{d[\delta P(\mathbf{r}_{n'}, t')]}{dt'} dt'. \tag{35}$$

Taking into account the relations (28), (29), (33), (34) and (35) and after some algebra, one obtains for the spectral differential scattering cross section (with $\Phi = \pi/2$)

$$\frac{d^2\sigma}{d\Omega d\omega_f} = \frac{1}{8\pi^2 c^4} \omega_i \omega_f^3 [n(\omega) + 1] \hbar \sum_j |a_j|^2 \frac{1}{2\omega_j} [\delta(\omega - \omega_j) - \delta(\omega + \omega_j)] \tag{36}$$

with

$$a_j = \sum_{\alpha, n} \frac{\chi_{\alpha n}}{\sqrt{m_n}} e_{\alpha n}(j) \exp(i\mathbf{q}_d \cdot \mathbf{r}_n). \tag{37}$$

$\omega > 0$ ($\omega < 0$) correspond to photon energy loss (gain). The Stokes components are associated with $\omega > 0$ while the anti-Stokes components are associated with $\omega < 0$ (Hayes and Loudon 1978). \mathbf{q}_d is the momentum transfer. ΔV has been included in the definition of susceptibility derivatives.

Determination of (36) and (37) requires the calculation of eigenfrequencies and eigenvectors of the dynamical matrix, which is not easy for large systems without perfect periodicity. Usual diagonalization fails for systems greater than about some thousand atoms. Since it is necessary to calculate the spectrum for very large systems, we used the spectral moments method. By this method we extract, directly from the dynamical matrix, only the active modes in the processes studied, with the correct intensity. A new function is introduced, which is equal to (36) for $\omega > 0$, but is symmetrical

$$g^R(u) = \frac{d^2\sigma}{K_0 d\Omega d\omega_f} = \sum_j \frac{|a_j|^2}{2\omega_j} [\delta(\omega - \omega_j) + \delta(\omega + \omega_j)] = \sum_j |a_j|^2 \delta(u - \lambda_j) \tag{38}$$

with

$$K_0 = (1/8\pi^2 c^4) \omega_i \omega_f^3 [n(\omega) + 1] \hbar.$$

Knowledge of (38) allows determination of the scattered intensity. Now for the calculation of $g^R(u)$ we introduce the vectors $|v\rangle$ such that

$$|v\rangle = \sum_{\alpha, n} \frac{\chi_{\alpha n}}{\sqrt{m_n}} \exp(i\mathbf{q}_d \cdot \mathbf{r}_n) |\alpha n\rangle \tag{39}$$

in the site representation $|\alpha n\rangle$. Then the moments of $g^R(u)$ are directly obtained from the dynamical matrix D :

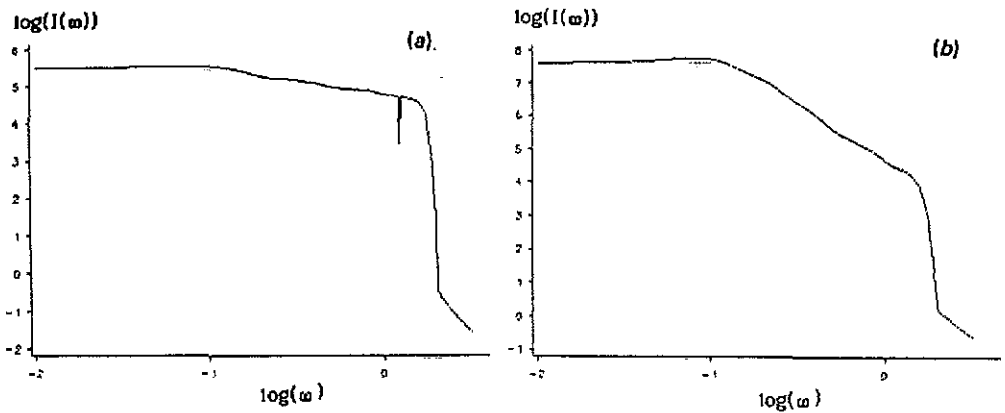


Figure 14. Log-log plot of the Raman intensity of the vectorial disordered ($n = 12$ level) Sierpinski gasket, with (a) random local Raman tensor and (b) local Raman tensors given as $\chi_{\alpha n} = (-1)^n$.

$$\mu_n^R = \int g^R(u) u^n du = \langle v | D^n | v \rangle. \quad (40)$$

From the moments, the scattering cross section itself is calculated (Benoit 1987, Benoit and Poussiguet 1989). From the invariance of the system as a whole, the coefficients $\chi_{\alpha n}$ are such that

$$\sum_n \chi_{\alpha n} = 0 \quad \text{for all } \alpha. \quad (41)$$

The exact structure of the system, density of states, localization (or super-localization) are taken into account without any special conjectures.

We have computed the Raman spectra for the disordered vectorial Sierpinski gasket (level $n = 12$) and, in order to compare our results concerning the scattering of light with previous experiments, we assumed that the distances between the atoms were equal to 30 \AA . The size of the gasket was $1.23 \mu\text{m}$. Two types of local Raman tensors and several scattering vectors were considered. Computation was performed with four scattering angles $\theta_d = 30^\circ, 90^\circ, 150^\circ$ and 180° . The results showed that the Raman spectra did not change much when the scattering angle was changed from 30° to 180° , which is in agreement with the experimental results.

We also computed the Raman intensity for several types of susceptibility derivatives (local Raman tensors) $\chi_{\alpha n}$. In the first model, the local Raman tensors are given by $\chi_{\alpha n} = \gamma_n$ where the γ_n are random variables distributed between -0.5 and 0.5 with a uniform probability density. Results are shown in figure 14(a). The spectrum over the cross-over frequency was a straight line with a slope of -0.78 . In the second model the local Raman tensors were given as $\chi_{\alpha n} = (-1)^n$. The Raman scattering spectrum is reported in figure 14(b). The slope of the curve over the cross-over frequency was then -3.32 .

5. Discussion and conclusions

Let us consider the results obtained for localization of the modes (figures 10 to 13). As already mentioned, we observed that the modes are much more localized in the

high-frequency regions for all models. We also note that, whatever the model, localized and non-localized modes appear in all the spectra. We should point out that a method used here takes into account the contribution of all modes with a given frequency (relation (24)) and concerning the atom n_c of the 'centre' of the gasket. Instead, we obtained the localization of a wavepacket around a given frequency and so the method gave an order of magnitude for average values of the localization of modes with a frequency between ω and $\omega + d\omega$ (or u and $u + du$). From the particular position of the atom n_c , part of the modes may have a zero component. For instance, from the symmetry, in the scalar model, the A_2 modes will have a zero component. However, for the disordered systems all modes may have a non-zero component on this atom. To obtain more information on the localization, we used the correlation function (7) to compute the localization ratio with the same atoms as used for the determination of $P(u)$ (relation (27)). For large ξ the value of the localization ratio was found close to 200. Now if the eigenmodes are not centred on the atom n_c the localization ratio can be larger than 200. So if $P(u)$ is smaller than about 200 the modes are certainly localized, and on the contrary the modes are extended and not centred on n_c .

For the perfect scalar model (figure 10) we find a strong localization for the $u = 3$ and $u = 6$ modes, which is in general agreement with the value obtained by Rammal (1984). We note that the localization decreases with the frequency.

For the disordered scalar model (figure 11), with the maximum frequency of the DOS being 5.32, we noted that the high-frequency modes are strongly localized, the localization ratio is practically zero up to $u = 3.55$, and that generally the modes are much more localized than for the perfect model. However, if some modes are strongly localized, we note the presence in all the spectrum of some extended modes. The conclusion is that the disorder in the scalar model for the Sierpinski gasket did not strongly disturb the low-frequency modes but is much more sensitive in the high-frequency region. This result is in agreement with the permanence of the discrete nature of the low-frequency spectrum, even with a strong disorder and also with the very nice fracton dispersion found with this model (figure 4).

For the perfect vectorial gasket we note that, in contrast to the perfect scalar model, in the high-frequency region (figure 12), the localization increases as the frequency decreases. The localization of the modes near the maximum frequency at $u = 4.79$ is not specially strong.

For the disordered vectorial Sierpinski gasket, with the maximum frequency of the spectrum being $u = 3.7$ (figure 13), we find a very strong localization in the high-frequency part (up to 3.16) and a strong localization of all modes over all the spectrum. The most interesting point concerned the presence of two different regions (figure 13(b)), which correspond exactly to both regimes found in the DOS (figure 9(b)). While in the low-frequency regime the localization ratio is a constant on much of the spectrum, the high-frequency regime is a succession of more or less localized modes. The strong localization of the low-frequency regime confirms that $g(\omega) \sim \omega$ law did not correspond to a genuine acoustic regime and this result explains why we did not obtain any dispersion of fractons with the vectorial disordered model: the modes are so localized that they are not affected by the change of the boundary conditions. It is not clear why one obtains a pseudo-Debye law in this system. The $\omega \rightarrow 0$ asymptotic behaviour of the DOS has been intensively studied in random one-dimensional systems (Dyson 1953, Alexander *et al* 1981 and references therein). These latter authors have shown that the exact behaviour depends on the class of

the probability density for the force constants. Very few studies have been carried out for higher-dimensional systems. The presence of a possible additional cross-over has been mentioned by Feng (1985), the elasticity being dominated by stretching at small scales and by bending at larger. However, the cross-over found here arises from the disorder and it is rather hard to define stretching or bending modes in our model. However, we note that the behaviour of the DOS did not depend on the form of the probability density, that the part of the spectrum concerned is small ($\omega_{co} \approx 0.1$, which gave $u_{co}/u_{max} \approx 1/400$), that the system was strongly disordered and that the modes were largely localized. If we consider an ensemble of systems with the same structure, for a given mode j , the squared frequency u_j is a function of the force constants k_l that concern this mode:

$$u_j = f_j(k_1, k_2, k_3, \dots, k_l, \dots, k_n) \quad j = 1, 2, 3, \dots, N \quad (42)$$

where the form of the functions f_j only depends on the structure.

Now the probability of finding u_j between u and $u + du$ is equal to the probability of finding k_1 between k_1 and $k_1 + dk_1$ multiplied by the probability of finding k_2 between k_2 and $k_2 + dk_2$ and so on, followed by a summation over all possible values of $k_1, k_2, k_3, \dots, k_l, \dots, k_n$ that satisfy the relation (42) with $u_j \in (u, u + du)$. The density of states can be written

$$G(u) = \sum_j \int p(k_1) dk_1 \int p(k_2) dk_2 \dots \delta(u - f_j(k_1, k_2, \dots)) \quad (43)$$

where the summation over j takes into account the possible contribution of the density of states for all modes at the squared frequency u . From statistical mechanics, it is well known that the average density of states will be equivalent to the DOS of an infinite isolated system. Now we can imagine that for strongly connected systems, in low-frequency regions, as u increases, the contribution of some modes (which should have a low frequency with all force constants equal to 1 for instance) decreases while the contribution of some other modes (which should have a higher frequency) increases. Such an effect may produce a constant density of states $G(u)$ and a linear form for $g(\omega)$ for a narrow zone of the spectrum. The same type of interpretation can be made for the localization ratio. The form of the component $e_{an}(j)$ of a mode j as a function of the force constants only depends on the structure or connectivity. The localization of this mode (value of the $e_{an}(j)$) will depend on the effective values of the elastic constants. It follows that, for a given frequency, many different modes with various localization lengths, even for a mode with a given type, will contribute to the correlation function (24), given a constant value of the localization ratio over a large region of the low-frequency part of the spectrum. Clearly such an interpretation needs to be confirmed. Let us note that an additional cross-over in the density of states of the fracton regime has been found recently in silica aerogels (Vacher *et al* 1990), which is interpreted as the presence of two distinct elastic regimes. We see that an alternative interpretation is that this cross-over could arise from disorder. We will now consider the fracton dimensionality obtained from the fracton dispersion and from the slope of the DOS in the fracton regime (table 2). For the perfect scalar model, the value obtained was close to the values obtained by Alexander and Orbach (1982), Rammal and Toulouse (1983) and Rammal (1984). The values obtained for the disordered model by both methods were in agreement. These values were slightly higher than those obtained with the perfect model. This result confirms the relatively weak effect of disorder on the dynamics of this system.

For the vectorial models, we had no relations between the values obtained from the fracton dispersion in the perfect lattice and from the DOS in the disordered one. In the strongly disordered Sierpinski gasket, the localization length $\xi(\omega)$ is no greater than the length L (relation (5)) and this certainly affects the fractal dimensionality. But it is not clear why these values were so different and why the values obtained with the disordered vectorial model were so close to the values obtained with the scalar systems. Let us now consider the DOS of the perfect gaskets. It is clear that we did not obtain a simple power form (2) as predicted by Alexander and Orbach (1982), Rammal and Toulouse (1983) and Rammal (1984). For infinite gaskets, the DOS will always behave, for $\omega \rightarrow 0$, as in figures 3 or 6. From the structure of the gasket and in contrast with a compact system or percolation networks, we noted that the number of degrees of freedom could not be continually varied. However, we will see that it is possible practically to define fracton dimensionality. We started from a very large system, fractal or not, and we divided it into disconnected equal-sized blobs large enough to neglect the boundary conditions for compact materials or corresponding to weakly connected blobs for fractals. For each blob there was a lower non-zero vibration frequency $\omega(L)$ that was associated with the size L of the blob. The relation (3) showed that the integrated density of states follows a power law for these discrete frequency values in a large system. For the Sierpinski gasket, this means that, if we plot the value of the integrated density of states, the points with frequencies $\omega(L(n))$, where n is the stage, will be on a straight line with the fracton dimensionality as the slope (in log-log plot). Between these frequencies, the integrated density of states (IDOS) will be a (devil's?) staircase. For compact materials and for percolation networks, from the statistical average, the set of points $\omega(L)$ will be dense and we shall obtain a smooth curve for the IDOS:

$$G(\omega) \sim \omega^d. \tag{44}$$

The spectral moments method mainly performs well for computing the linear response of the system, which is a leading interest for physicists. Let us note that the relations (36) and (37) can be written

$$\frac{d^2\sigma}{d\Omega d\omega_f} \sim \sum_j \sum_{\alpha, \beta, n, N} \left(\frac{\chi_{\alpha n} \chi_{\beta, n+N}}{\sqrt{m_n} \sqrt{m_{n+N}}} e_{\alpha n}(j) e_{\beta, n+N}(j) \exp(-i\mathbf{q}_d \cdot \mathbf{r}_N) \right) \times \frac{1}{2\omega_j} [\delta(\omega - \omega_j) - \delta(\omega + \omega_j)] \tag{45}$$

with $\mathbf{r}_{n'} = \mathbf{r}_n + \mathbf{r}_N$ ($n' = n + N$).

The term in the large parentheses represents the Fourier transform of a correlation function between the quantities $(\chi_{\alpha n}/\sqrt{m_n})e_{\alpha n}(j)$ and $(\chi_{\beta, n+N}/\sqrt{m_{n+N}})e_{\beta, n+N}(j)$. In crystals, these correlation functions can be easily obtained. In very porous materials the problem is much more difficult. To interpret the light scattering of fractals, Alexander (1989) conjectured that $(\chi_{\alpha n}/\sqrt{m_n})e_{\alpha n}(j)$ is proportional to the density, which is certainly correct, and found a power law for the Raman intensity. Here we calculated the Raman spectra of the disordered vectorial gasket. It is difficult to make any detailed comparison with the experimental results. However, we can imagine a system of layered Sierpinski gaskets without interaction, with an incident beam of light polarized perpendicular to the plane of the gasket. Scattered light is collected in the plane of the gasket with the same polarization. Both models developed for the local Raman tensor corresponded to a gasket where the homogeneous

particles were not symmetrical with the plane of the gasket. The first (disordered) model corresponded to a disorder in the orientation of these particles, while in the second model the particles were oriented up and down, giving increases or decreases of the polarizability with their displacements respectively. Raman scattering being a collective effect, the method used here was certainly not quite correct. However, it is the best way to take into account the structure (and the density) of the system and the correct correlation functions.

We observed that we have obtained, with both models in the fracton regime, a power law with the value of the slope being highly dependent on the value of the susceptibility derivatives χ_{an} of the material (figure 14). We also note that, in the fracton regime, Raman intensity after correction of the Boltzmann factor is not simply $g(\omega)/\omega$. The Raman process directly selects the q_d component of the Fourier transform of $(\chi_{an}/\sqrt{m_n})e_{an}(j)$ (relation (37)). It is natural that the Raman intensity depends on the value of χ_{an} and q_d . However, only scaling arguments can explain the power law obtained with both models.

In conclusion, the results obtained on the Sierpinski gasket, which is a quite difficult model to compute, showed that the spectral moments method is a very high-performance tool for calculating the complete DOS of a system. Difficulties only appeared for very low frequencies where the method could not resolve the various peaks of the spectrum. However, in contrast with other techniques, we do not compute the DOS point by point. The complete spectrum was directly obtained, with very reasonable computing times, from the generalized moments. We now have the tools to study a model of silica aerogels as close as possible to physical reality.

Acknowledgments

We would like to thank E Courtens, J Pelous and R Vacher for useful discussions, for a critical reading of the manuscript and constructive suggestions. One of us (CB) wants to thank Dr S Alexander for a helpful discussion. We also thank M Durand from IBM France and G Urbach and M Battle from Centre National Universitaire Sud de Calcul (CNUSC Montpellier) for their great help on the computing aspects of this work.

This work was supported by IBM France and the Centre National Universitaire Sud de Calcul (Ministère de l'Education Nationale), contract C3NI (High Performance Computing).

References

- Alexander S 1983a *Phys. Rev. B* **27** 1541
- 1983b *Phys. Rev. B* **29** 5504
- 1989 *Phys. Rev. B* **40** 7953
- Alexander S, Bernasconi J, Schneider W R and Orbach R 1981 *Rev. Mod. Phys.* **53** 175
- Alexander S and Haveli E 1983 *J. Physique* **44** 805
- Alexander S and Orbach S 1982 *J. Physique Lett.* **43** L625
- Barnsley M F, Devaney R L, Mandelbrot B B, Peitgen H O, Saupe D and Voss R F 1988 *The Science of Fractal Images* ed H-O Peitgen and D Saupe (Berlin: Springer)
- Benoit C 1987 *J. Phys. C: Solid State Phys.* **20** 765
- 1989 *J. Phys.: Condens. Matter* **1** 335

- Benoit C and Poussigie G 1989 *High Performance Computing* ed J L Delaye and E Gelenbe (Amsterdam: North Holland) p 347
- Benoit C, Poussigie G and Azougarh A 1990 *J. Phys.: Condens. Matter* **2** 2519
- Benoit C, Royer E and Poussigie G 1992 *J. Phys.: Condens. Matter* **4** 3125
- Born M and Huang K 1956 *Dynamical Theory of Crystal Lattices* (Oxford: Clarendon)
- Bourbonnais R, Maynard R and Benoit A 1989 *J. Physique* **50** 3331
- Brook Harris A and Aharony A 1987 *Europhys. Lett.* **4** 1355
- Chu B 1974 *Laser Light Scattering* (New York: Academic)
- Courtens E, Pelous J, Phalipou J, Vacher R and Woignier T 1987 *Phys. Rev. Lett.* **58** 128
- Courtens E, Vacher R, Pelous J and Woignier T 1988 *Europhys. Lett.* **6** 245
- Courtens E, Vacher R and Stoll E 1989 *Physica D* **38** 41
- Derrida B, Orbach R and Kin-Wah Yu 1984 *Phys. Rev. B* **29** 6645
- De Vries P, De Raedt H and Lagendijk A 1989 *Phys. Rev. Lett.* **62** 2515
- Domany E, Alexander S, Bensimon D and Kadanoff L P 1983 *Phys. Rev. B* **28** 3110
- Dos Santos D I, Aegerter M A, Craievich A F, Lours T and Zarzycki J J 1987 *Non-Cryst. Solids* **95-96** 1143
- Dyson F J 1953 *Phys. Rev.* **92** 1331
- Feng S 1985 *Phys. Rev. B* **32** 5793
- Feng S and Sen P N 1984 *Phys. Rev. Lett.* **52** 216
- Grest G S and Webman I 1984 *J. Physique Lett.* **45** L1155
- Hayes W and Loudon R 1978 *Scattering of Light by Crystals* (New York: Wiley)
- Jackson J P 1962 *Classical Electrodynamics* (New York: Wiley)
- Lax M and Nelson D F 1971 *Phys. Rev. B* **4** 3694
- Levy Y E and Souillard B 1987 *Europhys. Lett.* **4** 233
- Maradudin A A 1969 *Lattice Dynamics (Progress in Physics)* (New York: Benjamin)
- Maradudin A A, Montroll E W, Weiss G H and Ipatova I P 1971 *Solid State Phys. Suppl.* **3**
- Maradudin A A and Vosko S H 1968 *Rev. Mod. Phys.* **40** 1
- Montagna M, Pilla O, Viliani G, Mazzacurati V, Ruocco G and Signorelli G 1990 *Phys. Rev. Lett.* **65** 1136
- Pelous J, Sauvajol J L, Woignier T and Vacher R 1990 *J. Physique* **51** 433
- Poussigie G and Benoit C 1990 *Phonons '89* (Singapore: World Scientific) p 165
- Poussigie G, Benoit C, Sauvajol J-L, Lere-Porte J-P and Chorro C 1991 *J. Phys.: Condens. Matter* **3** 8803
- Rammal R 1984 *J. Physique* **45** 191
- Rammal R and Toulouse G 1982 *Phys. Rev. Lett.* **49** 1194
- 1983 *J. Physique Lett.* **44** L13
- Schaeffer D W and Keefer K D 1986 *Phys. Rev. Lett.* **56** 2199
- Southern B W and Douchant A R 1985 *Phys. Rev. Lett.* **55** 966
- Tremblay A M S and Southern B W 1983 *J. Physique Lett.* **44** L843
- Tsujimi T, Courtens E, Pelous J and Vacher R 1988 *Phys. Rev. Lett.* **60** 2757
- Vacher R, Courtens E, Coddens G, Heidemann A, Tsujimi Y, Pelous J and Foret M 1990 *Phys. Rev. Lett.* **65** 1008
- Vacher R, Woignier T, Pelous J and Courtens E 1987 *Phys. Rev. B* **37** 6500
- Webman I J and Grest G S 1985 *Phys. Rev. B* **31** 1689
- Williams M L and Maris H J 1985 *Phys. Rev. B* **31** 4508
- Yakubo K, Courtens E and Nakayama T 1990 *Phys. Rev. B* **42** 1078
- Yakubo K and Nakayama T 1987 *Phys. Rev. B* **36** 8933
- 1989 *Phys. Rev. B* **40** 517